

Z-DIRECTION HEAT TRANSFER IN COMPOSITES HYBRIDISED WITH LARGE DIAMETER METALLIC PINS

G. Neale^{1*}, Y. Fu¹ and A. Skordos¹

¹ School of Aerospace, Transport and Manufacturing, Cranfield University, Wharley End, Bedford, MK43 0AL, UK

* Corresponding author (g.d.neale@cranfield.ac.uk)

Keywords: through-thickness reinforcement, hybridisation, multifunctionality, carbon fibre, benzoxazine

ABSTRACT

Continuous fibre reinforced polymer composites have a well-established track record of excellent structural performance but generally lack non-structural functionalities inherent in legacy materials like metals. As the range of applications for composites continues to expand beyond their traditional base in aerospace, and to meet ambitious 'Net Zero' targets, there is increasing demand for embedded functionality in composites, like electrical or thermal energy transfer, though which a multitude of other functionalities are derived. A particularly under addressed challenge is how to efficiently achieve significant z-direction (through-thickness) functionality, which is restricted by the planar nature of composite. Through-thickness reinforcement (TTR) is typically used to achieve improvements in out-of-plane structural performance but can be applied to the integration of hybridising elements, like metallics, that can impart desired functionality. Here we demonstrate that composite hybridisation by the addition of large diameter (2 mm) metallic pins positively affects the z-direction transfer of thermal energy through carbon-benzoxazine composite without adverse effects on in-plane mechanical performance. This work conducts extensive mechanical and thermomechanical characterisation of the carbon-benzoxazine composite and the metal-composite hybridised system which feeds into the development of an experimentally validated macroscale (ply-level) representative volume element (RVE) finite element (FE) model. The FE model captures both thermal energy transfer and thermomechanical behaviour of the hybridised system during operation. Results show that highly conductive pins significantly improve the local thermal conductivity and act to accelerate heat flow through the hybridised system, reducing thermal lag through-the-thickness.

1 INTRODUCTION

The drive towards embedding thermal functionality in composite structures is motivated by composites' lack of good thermal conductivity, inherent in metals [1]. This deficiency requires the addition of hybridising elements to impart desirable functionalities to the composite. Most approaches either add materials to the laminate interlayer or alter matrix/fibre constituents, resulting in improvements in-plane thermal functionality without much out-of-plane improvement [2]. Although TTR is primarily used to improve composite delamination resistance, it is also a useful hybridisation method capable of integrating functional elements for thermal/electrical management, sensing, electromagnetic interference shielding, etc. In relation to this work, z-direction thermal management remains a challenge across industrial markets due to harsh working environments and increasing heat dissipation demand from electronic devices. A specific example is in composite battery pack enclosures [3], where there is a need for excellent through-thickness thermal conductivity, currently necessitating either mostly metallic constructions and/or additional active cooling system capacity.

Existing hybridisation approaches used to improve thermal management, like metallic/graphite interlayers, focus on in-plane conductivity. Wu et al. [4] manufactured graphite sheet/carbon fiber hybrid composites and was able to achieve an in-plane thermal conductivity of $118.8 \text{ Wm}^{-1}\text{K}^{-1}$ but only managed to increase out-of-plane thermal conductivity by 23% up to $0.86 \text{ Wm}^{-1}\text{K}^{-1}$. However, the concept of using z-direction oriented elements to improve through-thickness thermal energy transfer is not new. Pegorin et al. [5] and Yu et al. [6] showed that an array of metallic z-pins in carbon/epoxy composite creates a conductive pathway in the through-the-thickness direction for rapid heat transfer. Li et al. [7], [8] investigated the synergistic effects of combining an array of z-pins with graphene

interlayers to affect both through-thickness and in-plane heat transfer in composites and was able to achieve a ~700% improvement in z-direction thermal conductivity in the system. The commonality with these approaches is that they all suggest a tight array (between 3 – 7 mm spacing) of z-pins to achieve z-pin volume fractions of up to 3%. A gap in knowledge exists here in understanding the heat transfer mechanisms and potential benefits when targeting z-direction heat transfer with much larger TTR elements rather than sub-millimetre ones (typically ~500 μm in diameter).

The benefits from this large diameter approach are: (i) increased cross-sectional areas, which is proportional to heat energy transfer, and (ii) better z-direction orientation control, due to increased stiffness of the pins that are less likely to bend and deform during manufacture. Established TTR methods are not capable of inserting pins of this size. However, previous work on the insertion of large diameter pins (>1 mm diameter) into woven prepreg stacks has proven a feasible and robust reinforcement process [9] which can provide accurate TTR element placement with low insertion forces and tow damage compared with existing methods for similar element sizes, like post-cure drilling. Moreover, it allows the integration of much larger, rigid elements whose integration is currently outside the envelope of applicability of existing TTR methods.

Here we demonstrate that composite hybridisation by the addition of large diameter (2 mm) metallic pins positively affects the local z-direction transfer of thermal energy through carbon-benzoxazine composite. This work conducts extensive mechanical and thermomechanical characterisation on the carbon-benzoxazine composite and hybridised system which feeds into the development of an experimentally validated macroscale (ply-level) RVE FE model. The work shows that hybridisation in this way does not have adverse local effects on in-plane mechanical performance and investigates, through simulation, the potential of this approach when applied to hybridisation materials with a range of thermal conductivities.

2 METHODOLOGY

2.1 Materials and Manufacturing

The prepreg system used in this work was 2 × 2 twill 12k (650 gsm) and 3k (200 gsm) BX180-220 carbon-benzoxazine prepreg manufactured by SHD Composite Materials Ltd. [10]. Metal TT pins for experimental trials were manufactured from 304L stainless steel [11] rods with diameters of 1.2, 1.5 and 2.0 mm. TTR insertion was carried out using a TA.HDplus Texture Analyser, which is a universal testing machine with a 1 kN load cell, a force resolution of 1N, and a displacement resolution of 0.001 mm. Metallic pins were inserted through prepreg stacks in accordance with the procedure presented in [9] and the hybridised system was cured according to the prepreg manufacturer's guidance.

2.2 Material Characterisation

Tension tests were conducted using an Instron 5500R universal testing machine in accordance with ASTM D3039 [12] at 23°C (room temperature) and 180°C for unpinned-tension specimens and ASTM D6742 [13] for pinned-tension specimens at room temperature only. The Boeing-modified ASTM D6742 [7] was used for pinned-compression specimens and Boeing-modified ASTM D695 [8] for unpinned-compression specimens. V-notch shear tests on unpinned-shear specimens were carried out according to D7078 [14] at 23°C (room temperature) and 180°C. Unpinned specimens for material characterisation at 23°C and 180°C fed into the FE model and consisted of a [0/90]₄ layup, whereas other pinned and unpinned specimens presented in the results consisted of a quasi-isotropic [0/90,±45]₈ layup. Thermal expansion coefficients were determined using a TA Instruments Discovery TMA 450 Thermomechanical Analyser (TMA) and thermal conductivity (λ) and heat capacity (C_p) were determined using a TA Instruments-Waters DLF-1200 Laser Flash Analyser (LFA) in accordance with ASTM E1461 [15].

2.2 Simulation

A ply-level thermomechanical finite element simulation consisting of a 12 mm × 12 mm representative volume element (RVE) capturing the local area around the pin was analysed in MSC

Marc. The RVE consists of three main components. They are the laminate, the pin, and a resin region at the pin-laminate interface. The laminate is modelled as 16-layers of full integration hex continuum elements, each corresponding to a layer of BX180-220. The average size and distribution of the elements is given in Figure 1. The pin was modelled as a $\phi 2.0$ mm cylinder using full integration hex continuum elements. A 0.09 mm interface was included at the pin-composite boundary that has the properties of the bulk resin. The laminate consists of equal numbers of $0/90^\circ$ and $\pm 45^\circ$ oriented plies and each layer of elements is assigned an orientation of (1 0 0) for $0/90^\circ$ plies and (1 1 0) for $\pm 45^\circ$ plies. As this preliminary work focuses on z-direction heat transfer, the model does not consider local in-plane yarn deviation due to insertion at the pin location and assumes no resin rich regions based on [9]. All material parameters used in the simulation are given in *Ambient temperatures during testing in round brackets.
**References to sources for property values in square brackets.

Table 1 or derived from experimental characterisation in Figure 3.

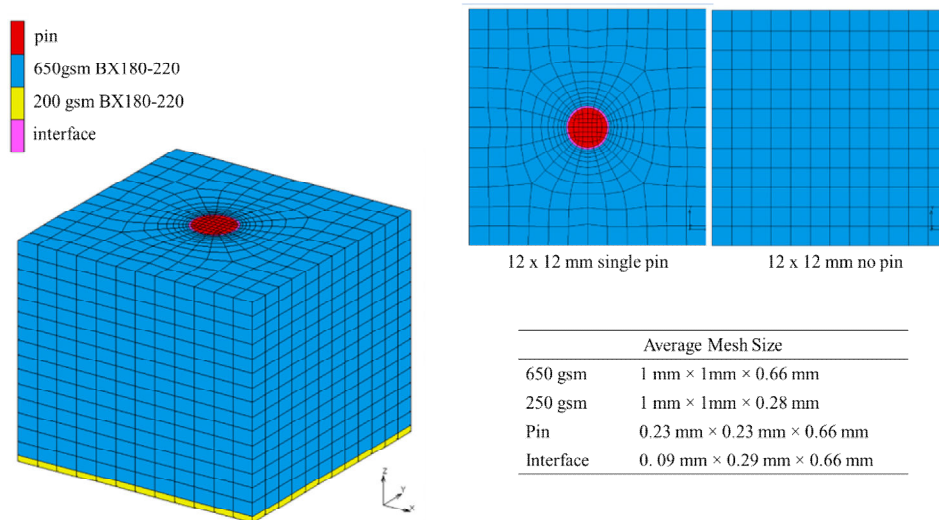


Figure 1: RVE specimens showing geometry and mesh used for analysis.

	Specific Heat capacity (J/(kg·K))	Density (kg/m ³)	Thermal Conductivity (W/(m·K))	Thermal Expansion ×10 ⁻⁶ (m/m·K)	Modulus (GPa)	Poisson's Ratio
Stainless steel	475 (25°C)	8010 [17]	14.9 (21°C)	16 (20°C) 17 (200°C) [17]	197 (20°C)	0.28 [17]
	485 (50°C)		15.1 (38°C)		197 (100°C)	
	505 (100°C)		16.1 (93°C)		187 (140°C)	
	520 (150°C)		17 (149°C)		185 (200°C)	
	530 (200°C)		18 (204°C)			
Carbon	800 [8]	1600 [8]	93 [8]			
Molybdenum	250 [18]	10200 [18]	142 [18]			
BX180-220 (650 gsm)		1584		x: 6.9	Young's: 49.5 (23°C) 48.2 (180°C)	0.22 (23°C)
			y: 4.9	Shear:	0.28 (180°C)	
			z: 40.7	11.3 (23°C)		
				11.1 (180°C)		

*Ambient temperatures during testing in round brackets.

**References to sources for property values in square brackets.

Table 1: Material Characterisation data input for FE simulation.

3 RESULTS AND DISCUSSION

3.1 Effect of z-direction hybridisation on mechanical performance

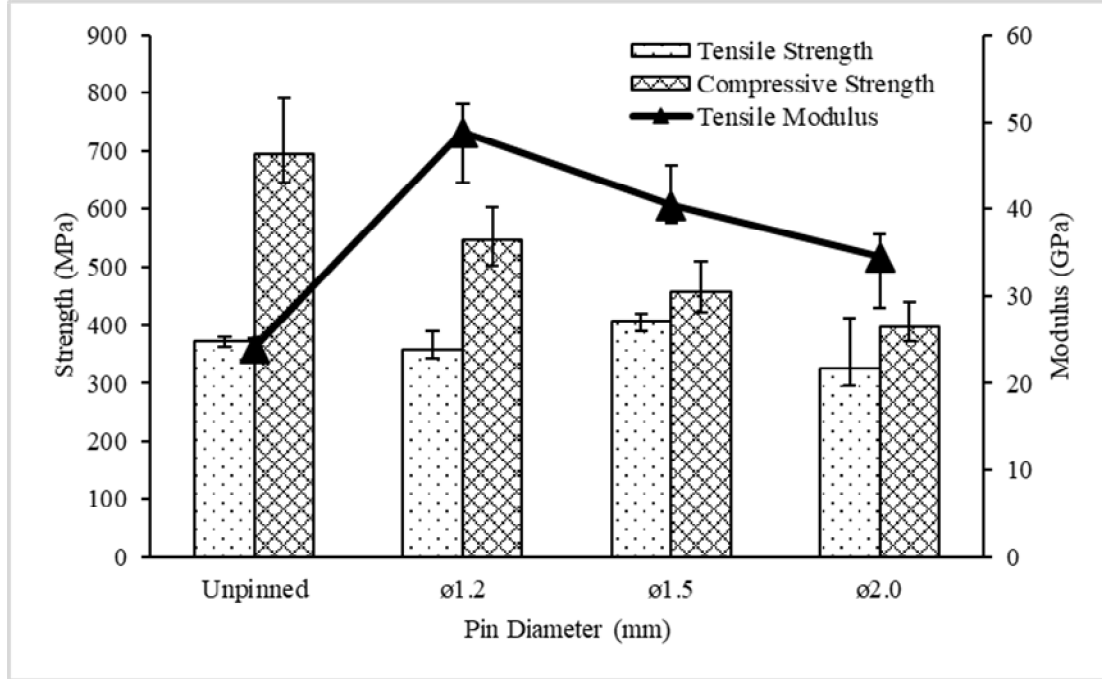


Figure 2: Variation of tensile and compression properties of pinned and unpinned specimens with respect to pin diameter.

Figure 2 shows the results of in-plane mechanical characterisation of pinned and baseline samples for $\phi 1.2$, $\phi 1.5$ and $\phi 2.0$ mm pin diameters. Tensile strength is unaffected by the presence of pins up to 2 mm diameter. Tensile failure transitions from delamination failure in baseline specimens to complete tow rupture in pinned samples. The presence of the pins therefore acts to suppress the delamination failure in the material and encourage higher energy tow rupture which balances the potential local degradation caused by the stress concentration at the pin, resulting in an unaffected tensile strength. Tensile modulus is improved by the presence of the TTR pins, doubling in 1.2 mm pinned samples. There is a significant degradation in compressive strength, increasing in severity with pin diameter to a maximum of a 42% reduction in 2.0 mm diameter pinned samples. Compressive strength in composites is known to be extremely sensitive to crimp and waviness. As pin diameter increases, local fibre crimp and waviness in the region immediately surrounding the pin increases. Although the static insertion method seems to do a good job of minimising this effect, both local tow disturbance and local volume fraction inevitably increase exponentially with pin diameter. This added waviness promotes interlaminar failures that shows signs of delamination buckling failure and subsequent splaying.

3.1 Thermal characterisation

For the thermomechanical evaluation and FE simulation work, this paper only considers $\phi 2.0$ mm pins. Figure 3 shows the results of thermal characterisation for the BX180-220 composite. Both thermal conductivity (λ) and specific heat capacity (C_p) in the 1-, 2-, and 3-directions increase with temperature. The figure also presents a rule of mixtures (RoM) estimation of the effective λ and C_p of the hybridised composite-pin system considering the RVE according to Equations 1 and 2 below.

$$\lambda_{\text{hybrid}} = v_{\text{pin}}\lambda_{\text{pin}} + v_{200\text{gsm}}\lambda_{200\text{gsm}} + v_{650\text{gsm}}\lambda_{650\text{gsm}} \quad (1)$$

$$C_{p \text{ hybrid}} = v_{pin} C_{p \text{ pin}} + v_{200gsm} C_{p \text{ 200gsm}} + v_{650gsm} C_{p \text{ 650gsm}} \quad (2)$$

Where λ is thermal conductivity, C_p is specific heat capacity and v is volume fraction. The RoM estimation shows that stainless steel pins increase the local thermal conductivity by up to 37% in hybridised system compared to the unpinned composite.

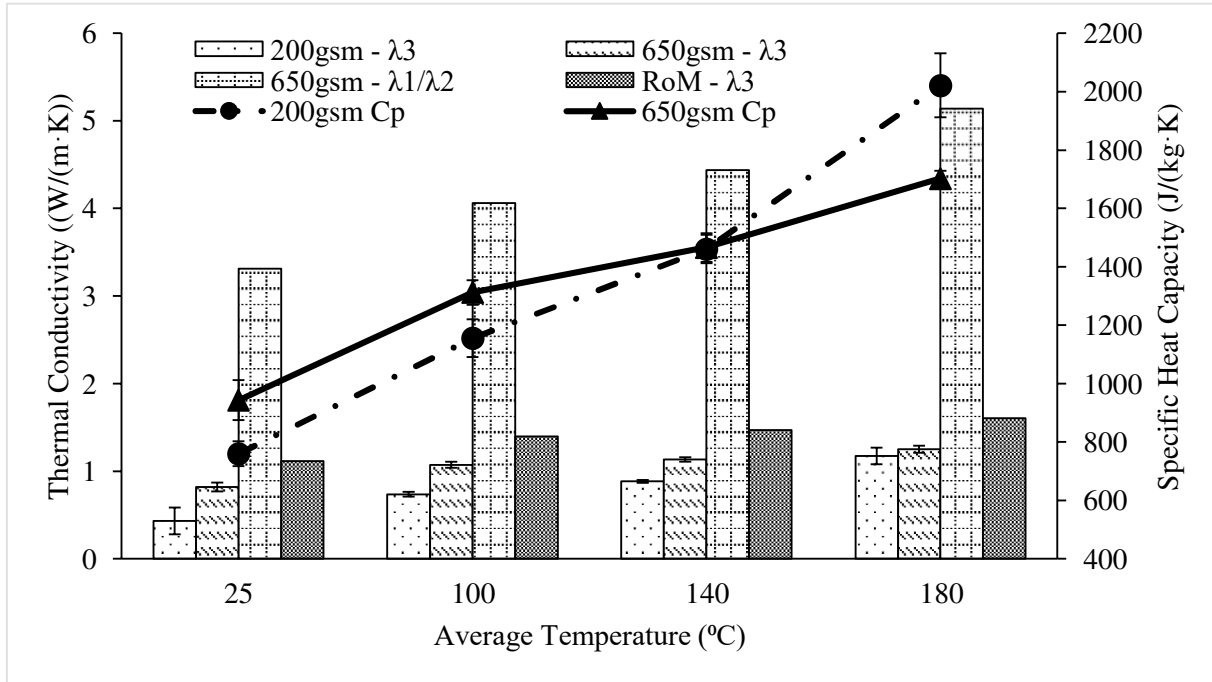


Figure 3: Thermal characterisation results.

A heat pulse was applied to the unpinned RVE model to simulate the LFA process and to validate the FE simulation. A boundary condition was set for a heat pulse on the lower surface of RVE model with a time length of 10^{-4} s and a heat flux of 3×10^7 W/m². By considering interfacial heat exchange in the FE simulation the time-dependent temperature change was obtained, and the simulated z-direction thermal diffusivity (α) was calculated according to Equation 3 [15].

$$\alpha = \frac{0.139L^2}{t_{1/2}} \quad (3)$$

Where α is thermal diffusivity, L is the z-direction thickness and $t_{1/2}$ is the period when the detected temperature reaches half of the maximum. Figure 4 compares the relationship between temperature and thermal diffusivity (α) for experimental and simulation results and shows good agreement between them.

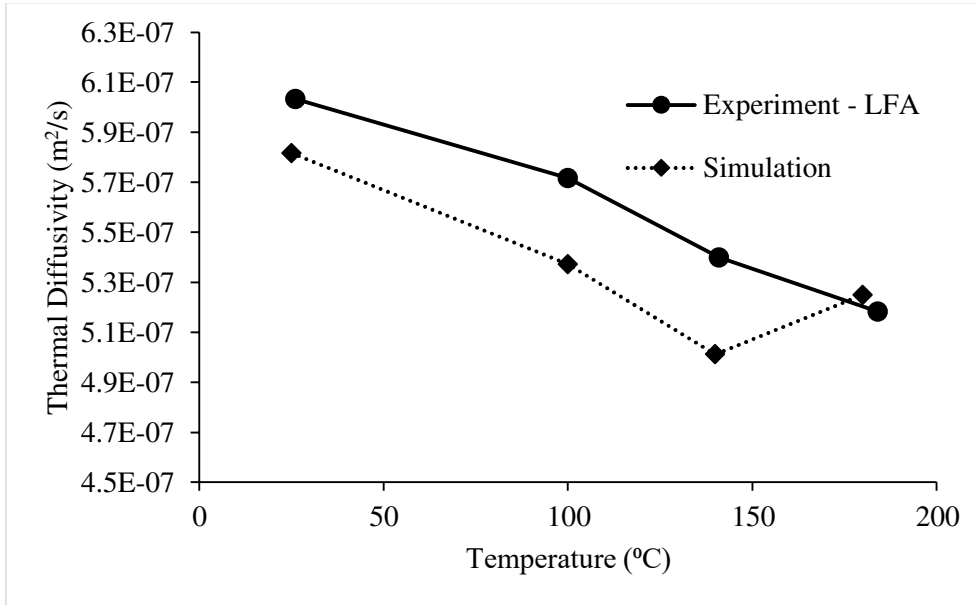


Figure 4: Graph showing experimental and simulated results for ambient temperature vs thermal diffusivity in unpinned composites.

3.2 Effect of hybridised system on heat transfer

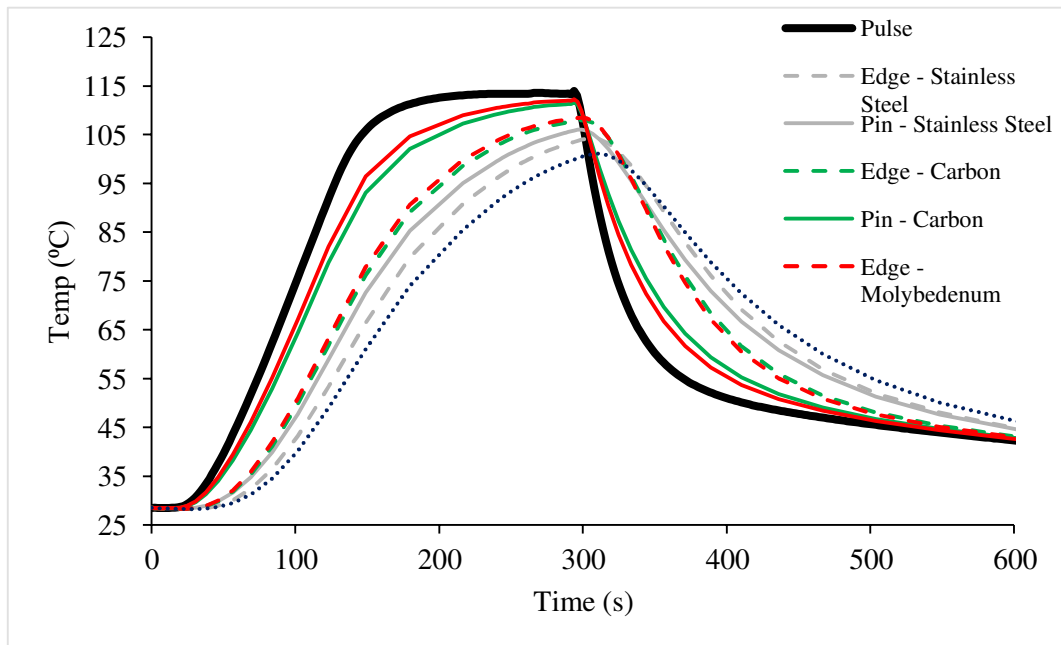


Figure 5: Transient heat response graph.

Figure 5 shows temperature versus time response graphs for a longer experimental transient heat pulse (black line) applied uniformly to the bottom surface of the RVE using the temperature profile recorded using thermocouples on a ceramic heating plate. The temperature ramps from room temperature (28 °C) up to a maximum of 115 °C. At 300 s, the heating plate is turned off. The z-direction heat transfer is captured by recording the temperatures at the top surface of the RVE at a node at the centre of the pin (solid lines) and at node away from the pin at the RVE edge (dashed lines). These and are used to track the time-temperature relationship for heat transfer through the thickness of the RVE. The experimental LFA method cannot be successfully applied here because the 16-layer composite is

too thick. The dark blue dotted line shows simulated time-temperature at top surface for unpinned composite.

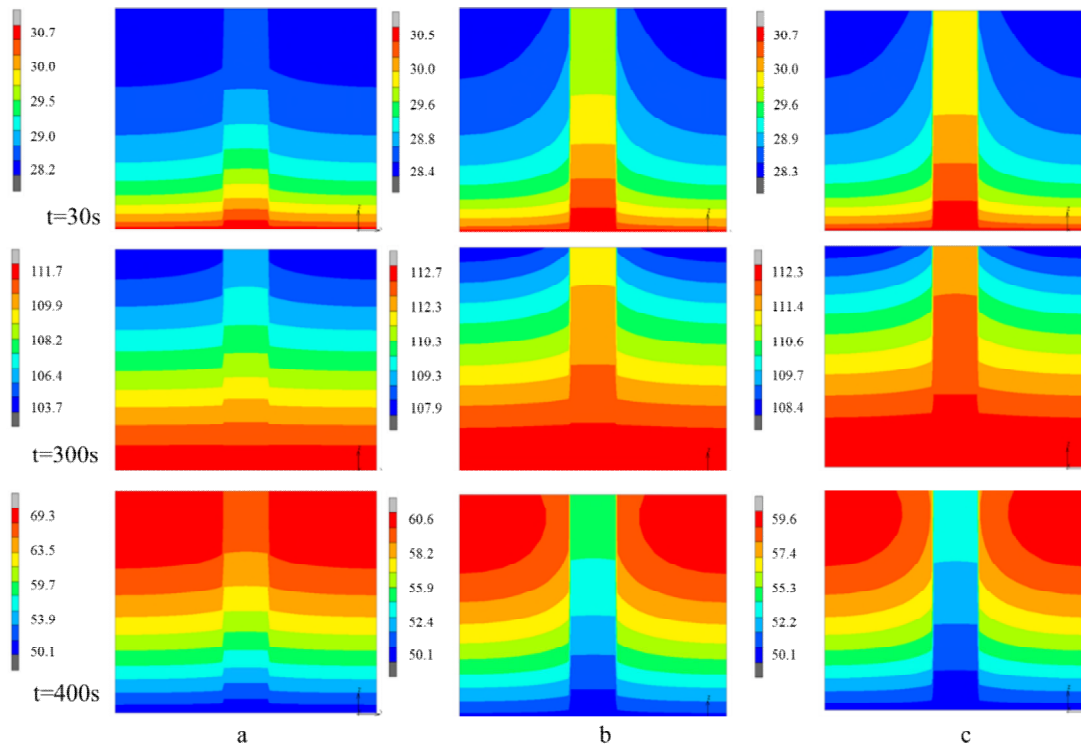


Figure 6: Cross-sectional temperature distribution for the (a) stainless steel, (b) carbon, and (c) molybdenum pins at different times during the application of the heat pulse in Figure 5. The heat pulse was applied to the bottom side of the laminates.

The grey, green, and red lines show the simulated results for stainless steel, carbon, and molybdenum pins, respectively. The simulation results show that the pins have a marked effect on heat energy transfer in the composite. There is a thermal lag between temperature at the bottom and top surfaces due to the time it takes for heat to move through the composite in the z-direction. In the unpinned composite, the peak temperature on the top surface (T_0) is 11 s behind and 14 °C lower than the input pulse. In stainless steel pinned composites, which has the lowest λ of the pin materials evaluated, the T_0 at the edge location moves upward (4 °C higher) and forward (6 s sooner) in pinned than in unpinned results. As the λ of the material increases, the thermal lag location narrows significantly. This is seen in molybdenum and carbon pins where the T_0 at the edge trends towards the pulse plot. The higher and earlier onset peak temperatures away from the pins in molybdenum and carbon pins supports more efficient heat transfer through the pinned system compared to the unpinned composite. Figure 6a, b, and c show the evolution of heat in RVEs pinned with stainless steel, carbon, and molybdenum pins, respectively. The images show that heat flow is fastest in the more conductive pins which transfer heat up and outwards during heating. At the input pulse peak ($t = 300$ s), the temperature at the centre of carbon and molybdenum pins is almost in equilibrium with the bottom surface. This is much improved on stainless steel pinned and unpinned results. During cooling in the carbon and molybdenum pinned composite (around $t=400$ s), it is observed that the pin cools faster than the surrounding composite. The contour plot shows that heat is absorbed into the pins, which function as heat sinks, and down and out through the bottom. This phenomenon is locally present in z-pinned composites but is much more pronounced here because of the much larger cross-sectional area which is 16 times larger (r^2 term in circle area equation) than a typical z-pin (diameter ~ 500 μm) and allows for greater heat energy transfer in accordance with the increasing of the area term in Equation 4.

$$\frac{Q}{A} = \frac{-\lambda\Delta T}{x} \quad (4)$$

Where Q is heat energy, A is cross-sectional area, λ is thermal conductivity, ΔT is temperature change and x is distance. One of the key benefits presented by pinning large diameter pins is that their high stiffness prevents bending and hence the deviation from being perfectly normal to the surface (i.e., more efficient conductive pathways) unlike in other through-thickness reinforcement methods like tufting, stitching and 3D weaving.

4 CONCLUSIONS

Thermomechanical characterisation of singular layers of the cured carbon-benzoxazine material are as expected and values for thermal conductivity (λ) and specific heat capacity (C_p) increase with increasing temperature. These material characterisation outputs, along with tension and shear characterisation data for the composite at room temperature (23°C) and 180°C fed into the finite element model for the representative volume element and analysed using MSC Marc. Simulation results for the composite agreed well with experimental characterisation results for thermal diffusivity.

The presence of the stainless-steel pins improves local z-direction heat transfer in the composite compared to the unpinned material as the pins act as a thermally conductive pathway for heat to move through the composite thickness. This reduces the time for heat dissipation through the material thickness. Pin materials with higher thermal conductivity, in this case carbon and molybdenum, are shown to achieve drastic improvements in local heat energy transfer, reducing time-temperature lag.

The novelty in this work is in the use of large diameter (> 1mm) through-thickness pins to achieve hybridisation that is capable of significantly affecting local heat energy transfer, not possible with existing methods like tufting, z-pinning, and stitching. The key contribution is that multifunctionality is introduced in this way with no reduction in planar tensile strength or modulus thanks to the successful application of the static insertion method. The potential impact stemming from this preliminary study is that localised improvement in heat transfer can be expanded to an array of similarly sized or larger pins which has positive implications for the use of this sort of through-thickness hybridisation for thermal management applications e.g., joule heating in thicker pins is more efficient.

ACKNOWLEDGEMENTS

This work was supported by the SEER project which has received funding from the European Union's Horizon 2020 research and innovation programme (Grant agreement 871875).

REFERENCES

- [1] G. Gardiner, "Aerocomposites: The move to multifunctionality," *Composites World*, 2015. Accessed: Aug. 01, 2022. [Online]. Available: <https://www.compositesworld.com/articles/aerocomposites-the-move-to-multifunctionality>
- [2] H. Mason, "Multifunctional composite structures across end markets," *Composites World*, 2021. Accessed: Aug. 01, 2022. [Online]. Available: <https://www.compositesworld.com/articles/multifunctional-composite-structures-across-end-markets>
- [3] H. Mason, "Designing a versatile, multi-material EV battery enclosure," *Composites World*, 2021. <https://www.compositesworld.com/articles/designing-a-versatile-multi-material-ev-battery-enclosure> (accessed Aug. 02, 2022).
- [4] G. C. Yu, L. Z. Wu, and L. J. Feng, "Enhancing the thermal conductivity of carbon fiber reinforced polymer composite laminates by coating highly oriented graphite films," *Mater Des*, vol. 88, pp. 1063–1070, Dec. 2015, doi: 10.1016/j.matdes.2015.09.096.
- [5] F. Pegorin, K. Pingkarawat, and A. P. Mouritz, "Numerical analysis of the heat transfer properties of z-pinned composites," *Composites Communications*, vol. 8, pp. 14–18, Jun. 2018, doi: 10.1016/j.coco.2018.03.002.

- [6] G. C. Yu, L. Z. Wu, L. J. Feng, and W. Yang, “Thermal and mechanical properties of carbon fiber polymer-matrix composites with a 3D thermal conductive pathway,” *Compos Struct*, vol. 149, pp. 213–219, Aug. 2016, doi: 10.1016/j.compstruct.2016.04.010.
- [7] M. Li, Z. Fang, S. Wang, Y. Gu, and W. Zhang, “Thermal conductivity enhancement and synergistic heat transfer of z-pin reinforced graphite sheet and carbon fiber hybrid composite,” *Int J Heat Mass Transf*, vol. 171, Jun. 2021, doi: 10.1016/j.ijheatmasstransfer.2021.121093.
- [8] M. Li, Z. Fang, S. Wang, Y. Gu, Y. Li, and Z. Zhang, “Thermal conductivity enhancement and heat transport mechanism of carbon fiber z-pin graphite composite structures,” *Compos B Eng*, vol. 172, pp. 603–611, Sep. 2019, doi: 10.1016/j.compositesb.2019.05.092.
- [9] G. Neale and A. Skordos, “Insertion of large diameter through-thickness metallic pins in composites,” *Mater Des*, vol. 216, p. 110559, Apr. 2022, doi: 10.1016/J.MATDES.2022.110559.
- [10] SHD Composites, “BX180-220 Benzoxazine Tooling Prepreg - Product Datasheet.” Jun. 21, 2017. Accessed: Jun. 21, 2021. [Online]. Available: <https://shdcomposites.com/admin/resources/bx180-220-pds.pdf>
- [11] Masteel UK Ltd., “Grade 304H Stainless Steel (UNS S30409),” Jul. 25, 2019. <https://www.azom.com/article.aspx?ArticleID=5050> (accessed Jul. 08, 2021).
- [12] ASTM, “D3039/D3039M: Standard Test Method for Tensile Properties of Polymer Matrix Composite Materials,” 2017. doi: 10.1520/D3039_D3039M-17.
- [13] ASTM, “D6742/D6742M – 17: Standard Practice for Filled-Hole Tension and Compression Testing of Polymer Matrix Composite Laminates,” 2015. doi: 10.1520/D6742_D6742M-17.
- [14] ASTM, “D7078/D7078M – 20’120’1 Standard Test Method for Shear Properties of Composite Materials by V-Notched Rail Shear Method 1,” 2020, doi: 10.1520/D7078_D7078M-20E01.
- [15] ASTM, “Standard Test Method for Thermal Diffusivity by the Flash Method,” 2013, doi: 10.1520/E1461-13R22.
- [16] D. P. Bentz and K. R. Prasad, “Thermal Performance of Fire Resistive Materials I. Characterization With Respect to Thermal Performance Models.” 2007. Accessed: May 03, 2023. [Online]. Available: <https://www.nist.gov/publications/thermal-performance-fire-resistive-materials-i-characterization-respect-thermal>
- [17] Y. Luo, W. Gu, W. Peng, Q. Jin, Q. Qin, and C. Yi, “A Study on Microstructure, Residual Stresses and Stress Corrosion Cracking of Repair Welding on 304 Stainless Steel: Part I-Effects of Heat Input,” *Materials 2020, Vol. 13, Page 2416*, vol. 13, no. 10, p. 2416, May 2020, doi: 10.3390/MA13102416.
- [18] Plansee, “Molybdenum.” <https://www.plansee.com/en/materials/molybdenum.html> (accessed May 05, 2023).

2023-08-04

Z-direction heat transfer in composites hybridised with large diameter metallic pins

Neale, Geoffrey

ICCM

Neale G, Fu Y, Skordos A. (2023) Z-direction heat transfer in composites hybridised with large diameter metallic pins. In: 23rd International Conference on Composite Materials (ICCM23), 30 July - 4 August 2023, Belfast, N. Ireland, UK

<https://iccm23.org/>

Downloaded from Cranfield Library Services E-Repository